

# Relaxation Patterns in Supercooled Liquids from Generalized Mode-Coupling Theory

Liesbeth M. C. Janssen,<sup>1,\*</sup> Peter Mayer,<sup>1,†</sup> and David R. Reichman<sup>1,‡</sup>

<sup>1</sup>*Department of Chemistry, Columbia University, 3000 Broadway, New York, New York 10027, USA*

(Dated: November 27, 2014)

The mode-coupling theory of the glass transition treats the dynamics of supercooled liquids in terms of two-point density correlation functions. Here we consider a generalized, hierarchical formulation of schematic mode-coupling equations in which the full basis of multipoint density correlations is taken into account. By varying the parameters that control the effective contributions of higher-order correlations, we show that infinite hierarchies can give rise to both sharp and avoided glass transitions. Moreover, small changes in the form of the coefficients result in different scaling behaviors of the structural relaxation time, providing a means to tune the fragility in glass-forming materials. This demonstrates that the infinite-order construct of generalized mode-coupling theory constitutes a powerful and unifying framework for kinetic theories of the glass transition.

The glass transition of liquids and dense colloidal suspensions represents one of the most puzzling phenomena in all of condensed matter science. Among the various theories of glass formation proposed in the last few decades, mode-coupling theory (MCT) has acquired a unique place in this area of research. In particular, MCT can reproduce important features of the time-dependent dynamics and relaxation of supercooled liquids using only static information as input, making it essentially the only theory of glassy dynamics based entirely on first principles [1, 2].

The main quantity of interest in MCT is the two-point density correlation function  $F(k, t) = N^{-1} \langle \rho_{-\mathbf{k}}(0) \rho_{\mathbf{k}}(t) \rangle$ , where  $\mathbf{k}$  is a wavevector with magnitude  $k$ ,  $\rho_{\mathbf{k}}(t)$  is the  $\mathbf{k}$ -th Fourier component of the spatial density fluctuations at time  $t$ ,  $N$  is the number of particles, and the brackets denote a canonical ensemble average. The equation of motion for  $F(k, t)$  contains a memory function that, within the standard MCT framework, is assumed to be dominated by pair-densities. This allows one to factorize the memory kernel, which is essentially a four-point density correlator, into a product of two two-point correlators. Applying additional Gaussian and convolution approximations for the static multi-point correlation functions subsequently yields a closed, self-consistent expression for the time evolution of  $F(k, t)$ .

One of the successes of standard MCT is its ability to capture the “cage effect” responsible for an intermediate-time plateau in correlation functions and the dramatic slow-down of dynamics upon decreasing the temperature or increasing the density. The scaling properties of  $F(k, t)$  associated with this  $\beta$ -relaxation process are also accurately reproduced. The power-law divergence of the  $\alpha$ -relaxation time ( $\tau$ ) predicted by MCT is consistent with experiments and computer simulations, but only in the mildly supercooled regime. A major drawback of the theory is that it predicts an ideal glass transition at relatively high temperatures or low densities. Furthermore, standard MCT cannot account for exponential (Arrhenius) or super-Arrhenius dependences of  $\tau$  in the deeply su-

percooled regime, and thus cannot describe distinct “strong” and “fragile” glass-forming behaviors, respectively [3].

In an effort to account for activated processes that round off the ideal MCT transition, Das and Mazenko [4] and Götze and Sjögren [5] extended standard MCT by considering additional perturbative couplings to current modes. Although this approach can improve the predicted behavior of standard MCT in the case of strongly supercooled liquids, it does not apply to (hard-sphere) systems undergoing Brownian motion, where current modes play no substantial role. Indeed, several recent theoretical and computational studies have disputed the importance of density-current mode coupling close to the glass transition on general grounds [6–8].

An alternative improvement to standard MCT, referred to as generalized MCT (GMCT), was first introduced by Szamel in 2003 [9]. GMCT relies on the fact that the exact time evolution of four-point density correlations is governed by six-point correlation functions, which in turn are controlled by eight-point correlations, and so on. This makes it possible to delay the factorization approximation for the memory kernel to a later stage. Numerical studies employing second- and third-order truncations have shown that GMCT indeed systematically improves the predicted MCT transition temperature (or volume fraction), implying that higher-order correlations account for at least some features ignored by standard MCT in the deeply supercooled regime [9, 10].

More recently, two of us extended the GMCT approach to *infinite* order using a simplified schematic model based on the form of the microscopic equations of motion, allowing the factorization closure to be rigorously avoided [11]. The general form of this infinite hierarchy reads (see Appendix A)

$$\dot{\phi}_n(t) + \mu_n \phi_n(t) + \lambda_n \int_0^t \phi_{n+1}(\tau) \dot{\phi}_n(t - \tau) d\tau = 0, \quad (1)$$

where the functions  $\phi_n(t)$  represent normalized  $2n$ -point density correlators ( $n \in \mathbb{N}$ ),  $\mu_n$  are generalized bare frequencies, and the  $\lambda_n = \lambda_n(\Lambda)$  parameters play the role of generalized inverse-temperature-like coupling constants. Here  $\Lambda$  can be thought of as the control parameter of the transition, e.g. inverse temperature or volume fraction. In arriving at the form of Eq. (1), we have employed Gaussian and convolution approximations for the static correlations, included only diagonal contributions to the memory functions, and treated all

\* Electronic mail: lmj2130@columbia.edu

† Current address: ThinkEco, Inc., 494 8th Avenue, New York, NY 10001, USA

‡ Electronic mail: drr2103@columbia.edu

wavevectors on an equal footing. These approximations are all similar to those employed in standard MCT. We emphasize that Eq. (1) is based on a fully microscopic theory, as detailed in Appendix A. In Ref. [11] we considered a simple hierarchy with  $\mu_n = n$  and  $\lambda_n = \Lambda$ , a constant, and found that it admits an analytic solution which is characterized by a continuously growing, exponentially diverging relaxation time. This result is to be contrasted with finite-order GMCT, which always predicts a power-law divergence at a sharp MCT transition. The inclusion of all multipoint dynamical correlations thus provides a means to strictly remove the sharp MCT transition and convert power-law divergences of  $\tau$  into exponentially varying forms.

In this article, we further elaborate on the infinite schematic GMCT framework and show that, by considering more general forms for the  $\mu_n$  and  $\lambda_n(\Lambda)$  parameters of the hierarchy, GMCT can account for a vast wealth of relaxation patterns in supercooled liquids. More explicitly, we demonstrate that infinite GMCT hierarchies can reproduce the many features of the standard-MCT-based  $F_2$  model—which is characterized by a sharp MCT transition and power-law relaxation [12, 13]—but can also reveal novel relaxation patterns beyond those predicted by standard MCT. We also discuss how both strong and fragile relaxation motifs can emerge within infinite GMCT hierarchies devoid of sharp transitions by tuning the  $n$ -dependence of the  $\lambda_n$ -parameters. This constitutes the first kinetic-theory-motivated framework that can account for different fragilities in glass-forming materials.

Let us first consider some general features of Eq. (1) and its solutions  $\{\phi_n(t)\}$ . An important quantity in our present discussion is the  $\alpha$ -relaxation time for the  $n$ -th level density correlator, which we define as

$$\tau_n = \int_0^\infty \phi_n(t) dt = \hat{\phi}_n(s=0). \quad (2)$$

Here  $\hat{\phi}_n(s)$  is the Laplace transform of  $\phi_n(t)$ , defined by  $\hat{\phi}_n(s) = \mathcal{L}\{\phi_n(t)\} = \int_0^\infty \phi_n(t) e^{-st} dt$ . By iterating the Laplace-transformed solution of Eq. (1) for  $s = 0$ , we obtain (see Appendix A)

$$\tau_n \simeq \frac{1}{\mu_n} \sum_{m=0}^{\infty} \prod_{i=0}^{m-1} \frac{\lambda_{n+i}}{\mu_{n+1+i}}. \quad (3)$$

Instead of considering the  $\alpha$ -relaxation time, one may also characterize the glass transition in terms of the long-time limit of  $\phi_n(t)$ . We define this long-time limit as  $q_n = \lim_{t \rightarrow \infty} \phi_n(t) = \lim_{s \rightarrow 0} s \hat{\phi}_n(s)$ , which can be written explicitly as (see Appendix A)

$$\frac{1}{q_n} = 1 + \frac{\mu_n}{\lambda_n} \frac{1}{q_{n+1}} \simeq \sum_{m=0}^{\infty} \prod_{i=0}^{m-1} \frac{\mu_{n+i}}{\lambda_{n+i}}. \quad (4)$$

Equations (3) and (4) are our general expressions for the relaxation time and long-time limit of  $\phi_n(t)$ , respectively, as governed by the infinite hierarchy of Eq. (1).

The convergence behavior of the general expressions (3) and (4) can already reveal important information on the type

of transition contained in the hierarchy. For an MCT-like transition, there exists a critical point  $\Lambda = \Lambda_c$  above which the  $\phi_n(t)$  no longer decay to zero. This nonzero long-time limit  $q_n$  may grow continuously (type-A transition) or discontinuously (type-B transition) as a function of the control parameter  $\Lambda$ . If the transition is completely avoided, the relaxation time grows continuously but ultimately leads to full relaxation of the correlation functions ( $q_n = 0$ ) for all finite  $\Lambda$ . One may verify that the series for  $\tau_n$  converges if  $\lim_{n \rightarrow \infty} \lambda_n / \mu_{n+1} < 1$ , and  $1/q_n$  converges if  $\lim_{n \rightarrow \infty} \mu_n / \lambda_n < 1$ . A type-A transition is characterized by a diverging series for both  $\tau_n$  and  $1/q_n$  at  $\Lambda = \Lambda_c$ , while a type-B transition has a diverging  $\tau_n$  series and converging  $1/q_n$  series. Conversely, for a rigorously avoided transition,  $\tau_n$  converges and  $1/q_n$  diverges for all  $\Lambda$ . Thus, depending on the asymptotic behavior of the  $\{\mu_n, \lambda_n\}$  coefficients, the GMCT framework can account for all of these physically distinct phenomena. This is one of the key results of this work: by making a suitable choice for  $\mu_n$  and  $\lambda_n$ , we can generate arbitrary types of transitions and, by virtue of Eqs. (3) and (4), arbitrary scaling behaviors of the relaxation time and long-time limit. The chosen set of  $\{\mu_n, \lambda_n\}$  coefficients subsequently determines the full hierarchy and all its time-dependent solutions  $\{\phi_n(t)\}$ .

In the remainder of this paper, we shall focus on some explicit examples of the general hierarchy (1) and restrict our discussion to the two-point density correlator  $\phi_1(t)$ , i.e.  $n = 1$ . All other correlation functions ( $n > 1$ ) appear only as generalized memory functions for  $\phi_1(t)$ . We first consider a class of hierarchies that exhibit MCT-like, type-B transitions but are fundamentally distinct from the standard-MCT  $F_2$  model. Note that the  $F_2$  model is essentially the lowest-order truncation of GMCT with closure  $\phi_2(t) = \phi_1^2(t)$  and  $\lambda_1 = 4\mu_1\Lambda$  [12]. We start with a relatively simple infinite hierarchy of the form  $\mu_n = n$  and  $\lambda_n = \Lambda(n + c)$ , where  $c \geq 0$ . The choice  $\mu_n = n$  follows naturally from the microscopic derivation of Eq. (1), provided that no explicit distinction is made between different wavevectors [11]. The functional form  $\lambda_n = \Lambda(n + c)$  implies that the coupling parameters  $\lambda_n$  also grow linearly with  $n$ , and will remain on the same order of magnitude as the frequencies  $\mu_n$  for all levels  $n$ . We obtain for the relaxation time  $\tau_1$  [see Eq. (3)]

$$\tau_1 = \sum_{m=0}^{\infty} \left( \prod_{i=1}^m \frac{i+c}{i+1} \right) \Lambda^m = \frac{1}{c\Lambda} \left[ \frac{1}{(1-\Lambda)^c} - 1 \right], \quad (5)$$

which diverges, to leading order, as  $\tau_1 \sim (1 - \Lambda)^{-c}$  near the critical point  $\Lambda_c = 1$ . Thus, our infinite hierarchy with parameters  $\{\mu_n = n, \lambda_n = \Lambda(n + c)\}$  predicts a *power-law* divergence of the  $\alpha$ -relaxation time, similar to the type-B transition in standard MCT. In fact, setting  $c$  equal to the standard-MCT  $\alpha$ -exponent  $\gamma \approx 1.765$  [12] yields exactly the same power-law behavior, implying that certain features of the schematic  $F_2$  MCT model can be accurately reproduced by a very simple infinite GMCT hierarchy.

Let us now consider the long-time limit of the density-density correlation function  $\phi_1(t)$  within this class of hierar-

chies. From Eq. (4), we find

$$\frac{1}{q_1} = \sum_{m=0}^{\infty} \left( \prod_{i=1}^m \frac{i}{i+c} \right) \left( \frac{1}{\Lambda} \right)^m. \quad (6)$$

Explicitly, for a hierarchy with  $c = 0$ , the inverse plateau height scales with  $\Lambda$  as  $1/q_n = \Lambda/(\Lambda - 1)$  for all  $n$ , the case  $c = 1$  gives rise to logarithmic scaling,  $1/q_1 = \Lambda \log[\Lambda/(\Lambda - 1)]$ , and for  $c = \gamma$  we have, for  $\Lambda \gtrsim 1$ ,  $1/q_1 = \frac{\gamma}{\gamma-1} \left( 1 + \frac{\pi(\gamma-1)}{\sin(\pi\gamma)} (\Lambda - 1)^{\gamma-1} + \mathcal{O}(\Lambda - 1) \right)$  (see Appendix B). In all cases,  $q_1 > 0$  for  $\Lambda > 1$ , confirming that these GMCT hierarchies induce something akin to type-B transitions at the critical point  $\Lambda_c = 1$  [1]. The expressions for  $q_1$  should, however, be contrasted with the  $F_2$  model [12], which predicts a *square-root* scaling of the form  $q_1^{F_2} = (1 + \sqrt{1 - 1/\Lambda})/2$ . Thus, standard-MCT-like hierarchies with  $\{\mu_n = n, \lambda_n = \Lambda(n + c)\}$  reveal entirely novel scaling behavior of the plateau height near the transition.

One may also ask whether it is possible to find an infinite hierarchy that exhibits *precisely* the same  $\Lambda$ -dependence as the  $F_2$  model, both with respect to  $q_1$  and  $\tau_1$ . A comparison between the Taylor series of  $1/q_1^{F_2}$  [Eq. (B9)] and Eq. (4) reveals that such an exact mapping requires

$$\frac{\lambda_n}{\mu_n} = \frac{2n+2}{2n-1} \Lambda. \quad (7)$$

By now fitting the  $\mu_n$  parameters such that they also reproduce the power-law relaxation time of the  $F_2$  model (see Appendix B), we obtain

$$\mu_n = \prod_{i=1}^{n-1} \frac{(2i+2)(i+b)}{(2i-1)(i+a)}, \quad (8)$$

with  $a \approx 0.52726$  and  $b \approx -0.23772$  determined numerically from the fit. Thus, an infinite GMCT hierarchy with coefficients (7) and (8) represents a numerically motivated approximation to the  $F_2$  model.

Figure 1 compares the functions  $\phi_1(t)$  obtained from the various MCT-like hierarchies discussed above, and from the exact  $F_2$  model [12], for different values of  $\Lambda$ . The GMCT hierarchies were truncated after  $N = 10000$  levels by exponential closure [ $\phi_N(t) = \exp(-Nt)$ ], which is amply sufficient to ensure convergence of the numerical solutions. All data were obtained using the time-integration algorithm of Fuchs *et al.* [14]. For all values of  $\Lambda$  considered, the hierarchy with  $\{\mu_n = n, \lambda_n = \Lambda(n + \gamma)\}$  exhibits clear deviations from the  $F_2$  model, yet exhibits exactly the same  $\tau_1$  power-law scaling. The numerically fitted GMCT hierarchy [Eqs. (7) and (8)], on the other hand, show almost perfect agreement with the exact  $F_2$  result, reproducing the complete time dependence of  $\phi_1(t)$  over all 6 decades of time. This is a remarkable and highly non-trivial result: by fitting only the  $\{\lambda_n, \mu_n\}$  parameters to a certain plateau height and relaxation time, we capture all qualitative and quantitative features of a finite-order schematic MCT model, both as a function of time and of  $\Lambda$ . We emphasize that no information of the short dynamics was included in the fit, and yet this time domain is also accurately described.

We thus argue that GMCT is indeed more general in the sense that it can successfully reproduce the predictions of standard MCT, but can also predict entirely novel transitions and relaxation patterns beyond those contained in the standard MCT scenario.

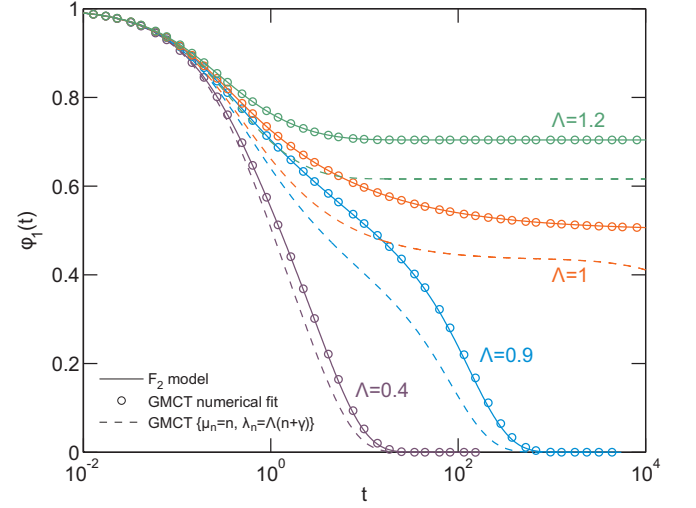


FIG. 1. Density-density correlation functions  $\phi_1(t)$  for the  $F_2$  model (solid lines), the fitted GMCT hierarchy with coefficients (7) and (8) (circles), and the GMCT hierarchy with  $\{\mu_n = n, \lambda_n = \Lambda(n + \gamma)\}$  (dashed lines), calculated for  $\Lambda = 0.4, 0.9, 1$  and  $1.2$ .

We now turn our attention to a different family of infinite GMCT hierarchies that are devoid of sharp MCT-like transitions. We will focus on hierarchical equations of the form  $\mu_n = n$  and  $\lambda_n = \Lambda n^{1-\nu}$ , with  $\Lambda, \nu > 0$ . Note that the infinite hierarchy with  $\mu_n = n$  and  $\lambda_n = \Lambda$ , which has already been discussed in Ref. [11], is a special case of this type of hierarchy. For this choice of parameters, the relaxation time becomes, after some manipulation (see Appendix C)

$$\tau_1(\Lambda) \sim \frac{(2\pi)^{(1-\nu)/2}}{\nu^{1/2}} \Lambda^{-\frac{\nu+1}{2\nu}} \exp(\nu \Lambda^{1/\nu}), \quad (9)$$

where we have assumed that  $\Lambda \gg 1$ . This assumption holds in the deeply supercooled regime, i.e. at asymptotically low temperatures. It is important to remark that, in contrast to the standard MCT prediction, the relaxation time of Eq. (9) does not diverge at any finite  $\Lambda$ . This implies that there is no sharp MCT transition at any finite  $\Lambda$  for an infinite GMCT hierarchy of the form  $\lambda_n = \Lambda n^{1-\nu}$ . Instead the relaxation time grows continuously with  $\Lambda$ , as was already found in Ref. [11] for the special case  $\nu = 1$ . It may be verified that the long-time limit of  $\phi_1(t)$  for this class of hierarchies also vanishes for all  $\Lambda, \nu > 0$ , confirming that the transition is rigorously avoided.

Let us look at some explicit examples of these avoided GMCT transitions. For  $\nu = 1$  ( $\lambda_n = \Lambda$ ), we recover the hierarchy of Ref. [11], with  $\tau_1(\Lambda) \sim \exp(\Lambda)/\Lambda$ . The case  $\nu = 2$  ( $\lambda_n = \Lambda/n$ ) yields (see Appendix C)  $\tau_1 = I_1(2\sqrt{\Lambda})/\sqrt{\Lambda}$ , where  $I_l$  is the modified Bessel function of the first kind. For large  $\Lambda$ , the relaxation time then behaves as  $\tau_1 \sim (4\pi)^{-1/2} \Lambda^{3/4} \exp(2\sqrt{\Lambda})$ , in accordance with Eq. (9).

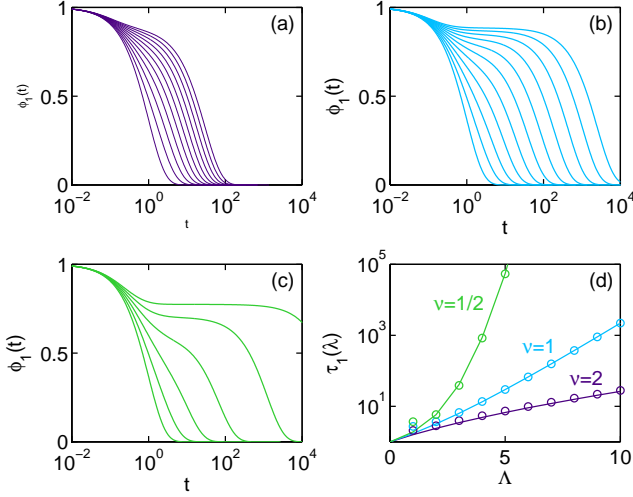


FIG. 2. Solutions  $\phi_1(t)$  of infinite hierarchies with  $\mu_n = n$  and  $\lambda_n = \Lambda n^{1-\nu}$  for (a)  $\nu = 2$  and  $\Lambda = 0, 1, \dots, 10$ , (b)  $\nu = 1$  and  $\Lambda = 0, 1, \dots, 10$ , (c)  $\nu = 1/2$  and  $\Lambda = 0, 1, \dots, 5$ . The fastest decaying functions correspond to  $\Lambda = 0$ . Panel (d) shows the associated relaxation times  $\tau_1(\Lambda)$ : the solid lines were obtained by numerical integration of  $\phi_1(t)$  over time [Eq. (2)], and the circles represent the analytical result of Eq. (9).

The density correlation functions  $\phi_1(t)$  for these two hierarchies, as well as those for  $\nu = 1/2$ , are shown in Fig. 2 for various values of  $\Lambda$ . The data have been obtained from numerical integration of the hierarchical equations using the algorithm of Ref. [14] with exponential closure at  $N = 1000$ . One can see that, for fixed  $\Lambda$ , the correlation functions decay more rapidly as  $\nu$  increases, as predicted by Eq. (9). This is the analog of the system become more fragile with increasing  $\nu$ . The difference in fragility between hierarchies with different  $\nu$  is best observed by examining the relaxation times  $\tau_1$  as a function of  $\Lambda$  [Fig. 2(d)]. These data were generated by numerically integrating the  $\phi_1(t)$  over time [Eq. (2)]. It is clear that hierarchies with small  $\nu$  give the most fragile behavior, i.e. the relaxation time increases more dramatically with varying  $\Lambda$  as  $\nu$  approaches zero. For comparison, we also show the analytical expression for  $\tau_1$  [Eq. (9)] in Fig. 2(d); the agreement with the numerical data is seen to be very good for  $\Lambda > 1$ . As a final point, we note that other features of  $\phi_1(t)$  are also affected by  $\nu$ , e.g. the plateau height of  $\phi_1(t)$  in the  $\beta$ -relaxation regime. In fact it has been noted that strong glass formers generally have larger plateau values compared to fragile ones [15]. The precise characterization of these features will be discussed in future work.

In the deeply supercooled regime, the true relaxation time diverges as an Arrhenius (exponential) or super-Arrhenius law, depending on the fragility of the system [3]. It is well established that standard MCT cannot account for such fragilities, and instead always predicts a power-law divergence of  $\tau_1$ . We find, however, that GMCT hierarchies of the form  $\{\mu_n = n, \lambda_n = \Lambda n^{1-\nu}\}$  ( $\Lambda, \nu > 0$ ) can account for different degrees of fragility depending on the value of  $\nu$ . This is an im-

portant result: the  $n$ -dependence of the coupling strengths  $\lambda_n$  in infinite-order GMCT provides a means to tune the fragility of a glass-forming system. While this finding is based on only a schematic description of the dynamics, one may expect it to be preserved in a fully microscopic version of GMCT, similar to how the qualitative features of the schematic  $F_2$  model are reproduced in  $\mathbf{k}$ -dependent standard MCT.

Finally, we briefly elaborate on the physical interpretation of the various GMCT hierarchies discussed in this work. First recall that the ratio  $\lim_{n \rightarrow \infty} \lambda_n / \mu_{n+1}$  determines whether the transition is sharp or avoided. For an avoided transition, the contributions of the higher-order memory kernels ultimately vanish at sufficiently large  $n$ , i.e. the couplings  $\lambda_n$  will become negligible compared to the bare frequencies  $\mu_n$ . Conversely, for sharp transitions, the  $\lambda_n$  always remain on the same order of magnitude as the frequencies  $\mu_n$  for all  $n$ . Thus, sharp MCT-like transitions contain significant contributions from *all* terms up to  $n \rightarrow \infty$ ; damping of the large- $n$  couplings will more strongly round off the MCT transition. For the class of avoided transitions studied here, with  $\lambda_n = \Lambda n^{1-\nu}$ , we see that the  $\lambda_n$  parameters decay more slowly with  $n$  as  $\nu$  decreases. This corresponds to a higher degree of fragility, and hence fragile systems are governed by relatively large contributions from higher-order dynamic correlations. In the limiting case  $\nu = 0$  we recover the linear hierarchy with  $c = 0$ , and the avoided transition turns into a sharp transition with (fragile) power-law relaxation. This is reminiscent of the MCT transition in the  $F_2$  model, which is generally believed to reflect a mean-field-like scenario. Thus, the ‘fragility’ parameter  $\nu$  might possibly be regarded as a measure for the mean-field (or MCT-like) character of the transition: the smaller the value of  $\nu$ , the more MCT-like the nature of system. An alternative interpretation of  $\nu$  follows from the notion that fragility is linked to microscopic structure, with more fragile systems exhibiting larger variations in short-ranged order than strong glass formers (see e.g. Ref. [16]). A stronger increasing dependence in  $\lambda_n$  (i.e. smaller  $\nu$ ) provides a means to increase the coupling between these structural motifs and the dynamics. For strong systems, it is expected that such intricate structural effects play a much smaller role in the relaxation dynamics. This could be captured in the GMCT hierarchy by rendering the coupling terms  $\lambda_n$  less important as the level  $n$  increases, i.e. by increasing  $\nu$ .

In summary, we have presented a schematic generalized mode-coupling theory in which dynamic multipoint density correlations are included through an infinite hierarchy of coupled equations. Such a hierarchical framework can accurately capture the many features of the standard-MCT  $F_2$  model, but can also give rise to generalized new forms of glass transitions, implying that there may be a purely dynamic origin for distinct glassy relaxation patterns. Moreover, a suitable choice of the coupling strengths of the higher-order correlations can lead to Arrhenius and super-Arrhenius behavior of the  $\alpha$ -relaxation time, providing a means to tune the degree of fragility with a single parameter. This represents the first MCT-based theory that can account for different fragilities in glass-forming materials.

## ACKNOWLEDGMENTS

LMCJ gratefully acknowledges support from the Netherlands Organization for Scientific Research (NWO) through a Rubicon fellowship, and from IMI-NFG (NSF grant DMR-0844014). DRR acknowledges grant nsf-che 1213247 for support.

## Appendix A: Microscopic and schematic GMCT equations

In this Appendix, we provide information on the microscopic ( $\mathbf{k}$ -dependent) foundation of our GMCT framework, and on the mathematical details of some of the schematic ( $\mathbf{k}$ -independent) GMCT results discussed in the main text.

Our schematic GMCT equations are based on a fully microscopic theory that accounts for the dynamics of the diagonal  $\mathbf{k}$ -dependent  $2n$ -point density correlation functions  $\phi_n(t)$ ,

$$\begin{aligned}\phi_1^{(k)}(t) &= \frac{\langle \rho_{-\mathbf{k}} \rho_{\mathbf{k}}(t) \rangle}{\langle \rho_{-\mathbf{k}} \rho_{\mathbf{k}} \rangle}, \\ \phi_2^{(k_1, k_2)}(t) &= \frac{\langle \rho_{-\mathbf{k}_1} \rho_{-\mathbf{k}_2} \rho_{\mathbf{k}_1}(t) \rho_{\mathbf{k}_2}(t) \rangle}{\langle \rho_{-\mathbf{k}_1} \rho_{-\mathbf{k}_2} \rho_{\mathbf{k}_1} \rho_{\mathbf{k}_2} \rangle}, \\ \phi_3^{(k_1, k_2, k_3)}(t) &= \frac{\langle \rho_{-\mathbf{k}_1} \rho_{-\mathbf{k}_2} \rho_{-\mathbf{k}_3} \rho_{\mathbf{k}_1}(t) \rho_{\mathbf{k}_2}(t) \rho_{\mathbf{k}_3}(t) \rangle}{\langle \rho_{-\mathbf{k}_1} \rho_{-\mathbf{k}_2} \rho_{-\mathbf{k}_3} \rho_{\mathbf{k}_1} \rho_{\mathbf{k}_2} \rho_{\mathbf{k}_3} \rangle}, \\ &\dots\end{aligned}\quad (\text{A1})$$

Each of these correlation functions is governed by an integro-differential equation with a memory kernel containing  $2(n+1)$ -point correlators. Assuming Gaussian factorization for the *static* correlations, we obtain for these memory kernels at level  $n$ ,

$$\begin{aligned}K_1(k, t) &= \frac{\rho k_B T}{16m\pi^3} \int d\mathbf{q} |V_{\mathbf{q}, \mathbf{k}-\mathbf{q}}|^2 S(q) S(|\mathbf{k}-\mathbf{q}|) \times \\ &\quad \phi_2^{(q, k-q)}(t), \\ K_2(k_1, k_2, t) &= \frac{\rho k_B T}{16m\pi^3} \sum_{i=1}^2 \frac{\mu_{k_i}}{\mu_{k_1} + \mu_{k_2}} \times \\ &\quad \int d\mathbf{q} |V_{\mathbf{q}, \mathbf{k}_i - \mathbf{q}}|^2 S(q) S(|\mathbf{k}_i - \mathbf{q}|) \times \\ &\quad \phi_3^{(q, k_1 - q\delta_{i1}, k_2 - q\delta_{i2})}(t), \\ K_3(k_1, k_2, k_3, t) &= \frac{\rho k_B T}{16m\pi^3} \sum_{i=1}^3 \frac{\mu_{k_i}}{\mu_{k_1} + \mu_{k_2} + \mu_{k_3}} \times \\ &\quad \int d\mathbf{q} |V_{\mathbf{q}, \mathbf{k}_i - \mathbf{q}}|^2 S(q) S(|\mathbf{k}_i - \mathbf{q}|) \times \\ &\quad \phi_4^{(q, k_1 - q\delta_{i1}, k_2 - q\delta_{i2}, k_3 - q\delta_{i3})}(t), \\ &\dots\end{aligned}\quad (\text{A2})$$

where for simplicity, and following Refs. [9, 10], we have retained only the diagonal dynamic contributions to the integral. In Eq. (A2),  $\rho$  denotes the total density,  $k_B$  is the Boltzmann constant,  $T$  is the temperature,  $m$  is the particle mass,  $V_{\mathbf{q}, \mathbf{k}-\mathbf{q}}$  are static vertices,  $S(q)$  is the static structure factor,  $\mu_{k_i} =$

$\frac{k_B T k_i^2}{m S(k_i)}$  is the bare frequency, and  $\delta_{ij}$  represents the Kronecker delta function. A detailed derivation of Eq. (A2), as well as its application to a realistic microscopic system, will be provided in a forthcoming publication. Following Ref. [11], we now drop the wavevector indices and treat all wavevectors on an equal footing. That is,  $\phi_1^{(k)}(t) \mapsto \phi_1(t)$ ,  $\phi_2^{(k_1, k_2)}(t) \mapsto \phi_2(t)$ ,  $\dots$ , and  $\mu_{k_1} + \dots + \mu_{k_n} \mapsto \mu_n$ . Note that  $\mu_n \propto n$  follows naturally if no distinction is made between different  $k$ -values. We also replace  $\frac{\rho k_B T}{16m\pi^3} \sum_{i=1}^n \int d\mathbf{q} |V_{\mathbf{q}, \mathbf{k}_i - \mathbf{q}}|^2 S(q) S(k_i - q)$  by a level-dependent constant  $n\lambda_n$ , which represents the effective weight of the memory kernel at level  $n$ . This brings the memory functions into the form  $K_n(t) \mapsto \lambda_n \phi_{n+1}(t)$ . Finally, we assume that the density correlation functions decay so slowly that the overdamped limit can be applied [ $\ddot{\phi}_n(t) = 0$ ]. Under these assumptions, we arrive at the generic schematic hierarchy of Eq. (1). These schematic GMCT equations are microscopically motivated, but lack any explicit  $\mathbf{k}$ -dependence. It is evident that Eq. (1) represents an infinite hierarchy of coupled equations, i.e., the time evolution of any  $\phi_n(t)$  is governed by  $\phi_{n+1}(t)$ , which in turn is governed by  $\phi_{n+2}(t)$ , etc. Equation (1) is subject to the initial conditions  $\phi_n(0) = 1$  for all  $n$ , which follows directly from the definitions of Eq. (A1).

The general solution of Eq. (1) may be written in terms of the Laplace transform as

$$\hat{\phi}_n(s) = \left( s + \frac{\mu_n}{1 + \lambda_n \hat{\phi}_{n+1}(s)} \right)^{-1}. \quad (\text{A3})$$

In order to find a general expression for the relaxation time [Eq. (2)], we can iterate Eq. (A3)  $k$  times for  $s = 0$  to yield

$$\tau_n \simeq \frac{1}{\mu_n} \sum_{m=0}^k \prod_{i=0}^{m-1} \frac{\lambda_{n+i}}{\mu_{n+1+i}} + \left( \prod_{i=0}^k \frac{\lambda_{n+i}}{\mu_{n+1+i}} \right) \tau_{n+k+1}. \quad (\text{A4})$$

This equation may be further simplified by a suitable choice of  $\mu_n$  and  $\lambda_n$  such that the second term will vanish for  $k \rightarrow \infty$ , and we arrive at Eq. (3) of the main text. Similarly, for the inverse plateau height we find by iteration

$$\frac{1}{q_n} = \sum_{m=0}^k \prod_{i=0}^{m-1} \frac{\mu_{n+i}}{\lambda_{n+i}} + \left( \prod_{i=0}^k \frac{\mu_{n+i}}{\lambda_{n+i}} \right) \frac{1}{q_{n+k+1}}, \quad (\text{A5})$$

where again the second term vanishes in the limit of  $k \rightarrow \infty$  if  $\mu_n$  and  $\lambda_n$  are chosen appropriately [Eq. (4)].

## Appendix B: Infinite GMCT hierarchies with standard-MCT-like behavior

Here we provide more mathematical details on the MCT-like infinite hierarchies discussed in the main text. We start with the hierarchy defined by

$$\begin{aligned}\mu_n &= n \\ \lambda_n &= \Lambda(n + c),\end{aligned}\quad (\text{B1})$$

with  $c \geq 0$ . As already mentioned in the main text, this type of hierarchy exhibits an MCT-like transition at the critical point

$\lambda_c = 1$ . For  $\Lambda > 1$ , the long-time limit of the  $2n$ -point density correlator  $\phi_n(t)$  satisfies

$$\frac{1}{q_n} = \sum_{m=0}^{\infty} \left( \prod_{i=1}^m \frac{n+i-1}{n+i-1+c} \right) \left( \frac{1}{\Lambda} \right)^m = {}_2F_1(1, n; n+c; 1/\Lambda), \quad (\text{B2})$$

where  ${}_pF_q(a_1, \dots, a_p; b_1, \dots, b_q; z) = \sum_{k=0}^{\infty} \frac{(a_1)_k \dots (a_p)_k}{(b_1)_k \dots (b_q)_k} \frac{z^k}{k!}$  is the generalized hypergeometric function with  $(x)_k$  the Pochhammer symbol [17]. For  $c = 0$ , this expression simplifies to

$$\frac{1}{q_n} = \sum_{m=0}^{\infty} \left( \frac{1}{\Lambda} \right)^m = \left( 1 - \frac{1}{\Lambda} \right)^{-1}, \quad (\text{B3})$$

which is independent of  $n$ . The case  $c = 1$  yields

$$\frac{1}{q_n} = \sum_{m=0}^{\infty} \left( \prod_{i=1}^m \frac{n+i-1}{n+i} \right) \left( \frac{1}{\Lambda} \right)^m = \sum_{m=0}^{\infty} \frac{n}{n+m} \left( \frac{1}{\Lambda} \right)^m, \quad (\text{B4})$$

which for  $n = 1$  becomes

$$\frac{1}{q_1} = \sum_{m=0}^{\infty} \frac{1}{1+m} \left( \frac{1}{\Lambda} \right)^m = \Lambda \log \left( \frac{\Lambda}{\Lambda-1} \right). \quad (\text{B5})$$

Thus, for a hierarchy with  $c = 1$ , the plateau height of the two-point density correlator  $\phi_1(t)$  grows logarithmically in the glassy regime. Let us now consider the special case  $c = \gamma$ , where  $\gamma \approx 1.76498$  is the standard-MCT exponent. As noted in the main text, this particular hierarchy exhibits a power-law divergence of the relaxation time with exponent  $\gamma$ , similar to the predictions of the  $F_2$  model. The expression for the (inverse) plateau height can be found by employing the series expansion of the hypergeometric function [Eq. (B2)], which yields for  $n = 1$  and  $\Lambda \gtrsim 1$

$$\frac{1}{q_1} = \Gamma(\gamma+1) \left\{ (\Lambda-1)^{\gamma-1} [\Gamma(1-\gamma) + \mathcal{O}(\Lambda-1)] + \frac{\Gamma(\gamma-1)}{[\Gamma(\gamma)]^2} + \mathcal{O}(\Lambda-1) \right\}, \quad (\text{B6})$$

where  $\Gamma(x)$  is the gamma function. Given that  $1 < \gamma < 2$ , we can isolate the leading term by writing

$$\begin{aligned} \frac{1}{q_1} &= \frac{\Gamma(\gamma+1)\Gamma(\gamma-1)}{[\Gamma(\gamma)]^2} \times \\ &\quad \left[ 1 + \frac{\Gamma(1-\gamma)[\Gamma(\gamma)]^2}{\Gamma(\gamma-1)} (\Lambda-1)^{\gamma-1} + \mathcal{O}(\Lambda-1) \right] \\ &= \frac{\gamma}{\gamma-1} \left[ 1 + \frac{\pi(\gamma-1)}{\sin(\pi\gamma)} (\Lambda-1)^{\gamma-1} + \mathcal{O}(\Lambda-1) \right]. \end{aligned} \quad (\text{B7})$$

Inverting this equation yields

$$\begin{aligned} q_1 &= \frac{\gamma-1}{\gamma} \left[ 1 - \frac{\pi(\gamma-1)}{\sin(\pi\gamma)} (\Lambda-1)^{\gamma-1} + \mathcal{O}(\Lambda-1) \right] \\ &= \frac{\gamma-1}{\gamma} \left[ 1 + \frac{\pi(\gamma-1)}{\sin[\pi(\gamma-1)]} (\Lambda-1)^{\gamma-1} + \mathcal{O}(\Lambda-1) \right]. \end{aligned} \quad (\text{B8})$$

Thus, for this type of hierarchy, the plateau height increases to leading order as  $(\Lambda-1)^{\gamma-1} \approx (\Lambda-1)^{0.765}$ .

It is well established that the  $F_2$  model predicts a long-time limit of  $\phi_1(t)$  that behaves as  $q_1^{F_2} = (1 + \sqrt{1-1/\Lambda})/2$  [12]. The Taylor series of  $1/q_1^{F_2}$  is given by

$$\frac{1}{q_1^{F_2}} = 1 + \sum_{m=1}^{\infty} \prod_{i=1}^m \left( \frac{2i-1}{2i+2} \right) \left( \frac{1}{\Lambda} \right)^m, \quad (\text{B9})$$

which can be compared with the general  $1/q_1$  expression for an arbitrary infinite GMCT hierarchy [Eq. (4)]. One may readily verify that an exact mapping between  $q_1^{F_2}$  and  $q_1$  requires for the GMCT coefficients

$$\frac{\lambda_n}{\mu_n} = \frac{2n+2}{2n-1} \Lambda. \quad (\text{B10})$$

A simple set of parameters satisfying this relation is  $\mu_n = n$  and  $\lambda_n = \Lambda \frac{2n(n+1)}{2n-1}$ . The  $\alpha$ -relaxation time associated with this hierarchy is

$$\begin{aligned} \tau_1 &= \sum_{m=0}^{\infty} \left( \prod_{i=1}^m \frac{2i}{2i-1} \right) \Lambda^m \\ &= \frac{\sqrt{\Lambda} \arcsin \sqrt{\Lambda} + \sqrt{1-\Lambda}}{(1-\Lambda)^{3/2}}, \end{aligned} \quad (\text{B11})$$

which diverges for  $\Lambda \rightarrow 1$  as  $\tau_1 \sim (\pi/2)(1-\Lambda)^{-3/2}$ . Note this divergence is slightly different from that predicted by standard MCT.

As a final example of  $F_2$ -like GMCT, we discuss the numerically fitted infinite hierarchy. In this case, we seek to (numerically) reproduce both the relaxation-time and plateau-height scaling of the  $F_2$  model by a suitable choice of  $\mu_n$  and  $\lambda_n$ . Since Eq. (B10) must hold, we can write for the relaxation time [see also Eq. (3)]

$$\tau_1 = \frac{1}{\mu_1} + \sum_{m=1}^{\infty} \frac{1}{\mu_{m+1}} \left( \prod_{i=1}^m \frac{2i+2}{2i-1} \right) \Lambda^m. \quad (\text{B12})$$

This series should be matched to the power law prediction of the  $F_2$  scheme, which diverges for  $\Lambda \rightarrow 1$  as

$$\begin{aligned} \tau_1^{F_2} &= \frac{A}{(1-\Lambda)^{\gamma}} \\ &= A \left[ 1 + \sum_{m=1}^{\infty} \left( \prod_{i=1}^m \frac{i+\gamma-1}{i} \right) \Lambda^m \right] \\ &\approx 1 + A \sum_{m=1}^{\infty} \left( \prod_{i=1}^m \frac{i+\gamma-1}{i} \right) \Lambda^m, \end{aligned} \quad (\text{B13})$$

The value of  $A \approx 1.2573$  has been obtained from a numerical fit of the  $F_2$  data close to the transition ( $\Lambda \lesssim 1$ ). Instead of working with Eq. (B12) directly, we now take the ansatz

$$\tau_1 = 1 + \sum_{m=1}^{\infty} \left( \prod_{i=1}^m \frac{i+a}{i+b} \right) \Lambda^m, \quad (\text{B14})$$

and seek to match the  $a$  and  $b$  constants to Eq. (B13). In the limit of  $m \rightarrow \infty$ , we have

$$\begin{aligned} \prod_{i=1}^{m-1} \frac{i+a}{i+b} &\sim \frac{\Gamma(1+b)}{\Gamma(a+1)} m^{a-b} \\ &\sim A \prod_{i=1}^{m-1} \frac{i+\gamma-1}{i}, \end{aligned} \quad (\text{B15})$$

which can be rewritten as

$$\frac{\Gamma(1+b)}{\Gamma(a+1)} m^{a-b} \sim A \frac{1}{\Gamma(\gamma)} m^{\gamma-1}. \quad (\text{B16})$$

Setting  $a = \gamma - 1 + b$  readily yields

$$A = \frac{\Gamma(\gamma)\Gamma(b+1)}{\Gamma(b+\gamma)}, \quad (\text{B17})$$

implying that  $b \approx -0.23772$  and  $a \approx 0.52726$ . This set of constants thus enforces that Eq. (B14) behaves as the MCT power law of Eq. (B13). A comparison between the ansatz (B14) and Eq. (B12) now gives for the  $\mu_n$  coefficients

$$\frac{1}{\mu_{n+1}} \left( \prod_{i=1}^n \frac{2i+2}{2i-1} \right) = \prod_{i=1}^n \frac{i+a}{i+b}, \quad (\text{B18})$$

or, more explicitly,

$$\mu_n = \prod_{i=1}^{n-1} \frac{2i+2}{2i-1} \frac{i+b}{i+a}. \quad (\text{B19})$$

The  $\lambda_n$  parameters subsequently follow from Eq. (B10), ensuring that also the plateau height  $q_1^{F_2}$  is correctly reproduced.

### Appendix C: Infinite GMCT hierarchies with avoided transitions

In this Appendix, we focus on the relaxation-time behavior of infinite hierarchies of the form  $\mu_n = n$  and  $\lambda_n = \Lambda n^{1-\nu}$ , with  $\Lambda, \nu > 0$ . This class of hierarchies lacks a sharp MCT-like transition for any finite  $\Lambda$ . Starting with Eq. (3) of the main article, we have

$$\tau_1 = \frac{1}{\mu_n} \sum_{m=0}^{\infty} \prod_{i=0}^{m-1} \frac{\lambda_{n+i}}{\mu_{n+1+i}} = \sum_{m=1}^{\infty} \frac{1}{\lambda_m} \prod_{i=1}^m \frac{\lambda_i}{\mu_i}, \quad (\text{C1})$$

which can be rewritten as

$$\begin{aligned} \tau_1 &= \sum_{m=1}^{\infty} \frac{1}{\Lambda m^{1-\nu}} \prod_{i=1}^m \frac{\Lambda i^{1-\nu}}{i} \\ &= \frac{1}{\Lambda} \sum_{m=1}^{\infty} \frac{1}{[(m-1)!]^\nu} \frac{\Lambda^m}{m} \\ &= \frac{1}{\Lambda} \sum_{m=1}^{\infty} \frac{1}{[(m-1)!]^\nu} \int_0^\Lambda x^{m-1} dx \\ &= \frac{1}{\Lambda} \int_0^\Lambda dx \sum_{m=0}^{\infty} \frac{x^m}{(m!)^\nu}. \end{aligned} \quad (\text{C2})$$

Introducing the function

$$f_\nu(x) = \sum_{m=0}^{\infty} \frac{x^m}{(m!)^\nu} \quad (\text{C3})$$

now yields for the relaxation time

$$\tau_1 = \frac{1}{\Lambda} \int_0^\Lambda f_\nu(x) dx. \quad (\text{C4})$$

For the special case  $\nu = 1$  we thus find  $f_1(x) = \sum_{m=0}^{\infty} x^m/(x!) = \exp(x)$  and  $\tau_1 = [\exp(\Lambda) - 1]/\Lambda$ , and for  $\nu = 2$  we have  $f_2(x) = \sum_{m=0}^{\infty} x^m/(x!)^2 = I_0(2\sqrt{x})$  and  $\tau_1 = I_1(2\sqrt{\Lambda})/\sqrt{\Lambda}$ , where  $I_l$  is the modified Bessel function of the first kind of order  $l$ .

In order to find a closed expression for  $\tau_1$  for arbitrary  $\nu > 0$ , we must evaluate the scaling behavior of  $f_\nu(x)$  as a function of  $\nu$ . This is a rather involved derivation; for simplicity we will focus on the asymptotic behavior for  $x \rightarrow \infty$  ( $\Lambda \rightarrow \infty$ ). We first approximate the sum in  $f_\nu(x)$  by an integral,

$$\begin{aligned} f_\nu(x) &\sim \int_0^\infty dm \frac{x^m}{\Gamma(m+1)^\nu} \\ &= \int_0^\infty dm \exp \left[ \log \left( \frac{x^m}{\Gamma(m+1)^\nu} \right) \right], \end{aligned} \quad (\text{C5})$$

and expand the logarithm up to second order around the point  $m = a$ ,

$$\begin{aligned} \log \left[ \frac{x^m}{\Gamma(m+1)^\nu} \right] &= \log(x^a \Gamma(a+1)^{-\nu}) + \\ &\quad \left[ \log(x) - \nu \psi^{(0)}(a+1) \right] (m-a) \\ &\quad - (\nu/2) \psi^{(1)}(a+1) (m-a)^2 + \mathcal{O}(m-a)^3, \end{aligned} \quad (\text{C6})$$

where  $\psi^{(i)}(x)$  is the polygamma function of order  $i$ , i.e. the  $(i+1)$ -th derivative of the logarithm of the gamma function. We will choose  $a = x^{1/\nu}$  so that the linear term in Eq. (C6) vanishes. Discarding the higher-order terms and extending the range of  $m-a$  to  $\pm\infty$  yields

$$\begin{aligned} f_\nu(x) &\sim \frac{x^a}{\Gamma(a+1)^\nu} \int_{-\infty}^{\infty} dm \exp \left[ -(\nu/2) \psi^{(1)}(a+1) m^2 \right] \\ &= \sqrt{\frac{2\pi}{\nu \psi^{(1)}(a+1)}} \frac{x^a}{\Gamma(a+1)^\nu}, \end{aligned} \quad (\text{C7})$$

where we have performed Gaussian integration. For  $a \rightarrow \infty$  we have, to leading order,  $\Gamma(a+1) \approx a^a \exp(-a) \sqrt{2\pi a}$  and hence

$$f_\nu(x) \sim \frac{(2\pi a)^{(1-\nu)/2} \exp(\nu a) x^a}{\nu^{1/2} a^{\nu a}}. \quad (\text{C8})$$

Substituting  $a = x^{1/\nu}$  finally yields

$$f_\nu(x) \sim \frac{(2\pi)^{(1-\nu)/2}}{\nu^{1/2}} x^{(1-\nu)/2\nu} \exp(\nu x^{1/\nu}). \quad (\text{C9})$$

One may verify that, for the special cases  $\nu = 1$  and  $\nu = 2$ , Eq. (C9) indeed describes the asymptotic behavior of  $f_1(x)$  and  $f_2(x)$ .

Finally, we seek to obtain a closed expression for the relaxation time  $\tau_1$  for general  $\nu > 0$ . Substituting Eq. (C9) into Eq. (C4) and setting  $y = \nu x^{1/\nu}$  gives

$$\tau_1 \sim (2\pi)^{(1-\nu)/2} \nu^{-\nu/2} \frac{1}{\Lambda} \int_0^{\nu\Lambda^{1/\nu}} dy y^{(\nu-1)/2} \exp(y), \quad (\text{C10})$$

which, by changing variables  $y \rightarrow \nu\Lambda^{1/\nu} - y$ , can be rewritten

as

$$\tau_1 \sim \frac{(2\pi)^{(1-\nu)/2}}{\nu^{1/2}} \Lambda^{-(\nu+1)/2\nu} \exp(\nu\Lambda^{1/\nu}) \times \int_0^{\nu\Lambda^{1/\nu}} dy \left(1 - \frac{y}{\nu\Lambda^{1/\nu}}\right)^{(\nu-1)/2} \exp(-y). \quad (\text{C11})$$

Expanding the power-law factor in the integrand and extending the integration range to  $+\infty$  finally yields, to leading order,

$$\tau_1 \sim \frac{(2\pi)^{(1-\nu)/2}}{\nu^{1/2}} \Lambda^{-(\nu+1)/2\nu} \exp(\nu\Lambda^{1/\nu}), \quad (\text{C12})$$

which is equivalent to Eq. (9) of the main article. Again it may be verified that this equation, which holds asymptotically for  $\Lambda \gg 1$ , is consistent with the expressions for  $\nu = 1$  and  $\nu = 2$  given earlier.

- 
- [1] W. Götze, Complex dynamics of glass-forming liquids: A mode-coupling theory (Oxford University Press, Oxford, 2009).
  - [2] L. Berthier and G. Biroli, *Rev. Mod. Phys.* **83**, 587 (2011).
  - [3] C. A. Angell, *Science* **267**, 1924 (1995).
  - [4] S. P. Das and G. F. Mazenko, *Phys. Rev. A* **34**, 2265 (1986).
  - [5] W. Götze and L. Sjögren, *Z. Phys. B* **65**, 415 (1987).
  - [6] M. E. Cates and S. Ramaswamy, *Phys. Rev. Lett.* **96**, 135701 (2006).
  - [7] A. Andreanov, G. Biroli, and A. Lefèvre, *J. Stat. Mech.* p. P07008 (2006).
  - [8] G. Szamel, *Prog. Theor. Exp. Phys.* p. 012J01 (2013).
  - [9] G. Szamel, *Phys. Rev. Lett.* **90**, 228301 (2003).
  - [10] J. Wu and J. Cao, *Phys. Rev. Lett.* **95**, 078301 (2005).
  - [11] P. Mayer, K. Miyazaki, and D. R. Reichman, *Phys. Rev. Lett.* **97**, 095702 (2006).
  - [12] E. Leutheusser, *Phys. Rev. A* **29**, 2765 (1984).
  - [13] U. Bengtzelius, W. Götze, and A. Sjölander, *J. Phys. C: Solid State Phys.* **17**, 5915 (1984).
  - [14] M. Fuchs, W. Götze, I. Hofacker, and A. Latz, *J. Phys.: Condens. Matter* **3**, 5047 (1991).
  - [15] J. Mattsson, H. M. Wyss, A. Fernandez-Nieves, K. Miyazaki, Z. Hu, D. R. Reichman, and D. A. Weitz, *Nature* **462**, 83 (2009).
  - [16] D. V. Louzguine-Luzgin, R. Belosludov, A. R. Yavari, K. Georgarakis, G. Vaughan, Y. Kawazoe, T. Egami, and A. Inoue, *J. Appl. Phys.* **110**, 043519 (2011).
  - [17] M. Abramowitz and I. A. Stegun, Handbook of Mathematical Functions (National Bureau of Standards, Washington, D.C., 1964).